Microbiological Research 290 (2025) 127959

Contents lists available at ScienceDirect

Microbiological Research

journal homepage: www.elsevier.com/locate/micres

Streptococcus anginosus orchestrates antibacterial potential of NETs facilitating survival of accompanying pathogens

Magdalena Pilarczyk-Zurek [a,1], Joanna Budziaszek [a,2], Keerthanaa Nandagopal [a], Aleksandra Kurylek [b,3], Aleksandra Kozinska [c,4], Michal Dmowski [b,5], Izabela Sitkiewicz [d,6], Izabela Kern-Zdanowicz [b,7], Joanna Koziel [a,*,8]

[a] *Department of Microbiology, Faculty of Biochemistry, Biophysics and Biotechnology of Jagiellonian University, Krakow, Poland*
[b] *Institute of Biochemistry and Biophysics, Polish Academy of Sciences, Warszawa, Poland*
[c] *Department of Drug Biotechnology and Bioinformatics, National Medicines Institute, Warszawa, Poland*
[d] *Institute of Biology, Warsaw University of Life Sciences-SGGW, Warszawa, Poland*

ARTICLE INFO

Key words:
Streptococcus anginosus
NETs
DNases
Virulence factor
Neutrophils
Coinfection
Enterobacteriales

ABSTRACT

Streptococcus anginosus is considered an emerging opportunistic pathogen causing life-threatening infections, including abscesses and empyema. Noticeably, clinical data revealed that *S. anginosus* also constitutes an important component of polymicrobial infections. Here, we showed for the first time that *S. anginosus* inactivates the antibacterial potential of neutrophil extracellular traps (NETs). The process is determined by a cell wall-anchored nuclease referred to as SanA, which high expression dominates in clinical strains isolated from severe infections. Nuclease activity protects *S. anginosus* against the antibacterial activity of NETs, supporting at the same time the survival of coexisting highly pathogenic species of *Enterobacteriales*. Obtained data suggest that SanA nuclease should be recognized as a critical *S. anginosus* virulence factor determining severe monospecies purulent infections but also shielding other pathogens promoting the development of polymicrobial infections.

1. Introduction

Streptococcus anginosus belongs to the *Streptococcus anginosus* Group (SAG). Those Gram-positive streptococci were classified for many years as commensal microbes colonizing the upper respiratory, digestive, and reproductive tracts (Asam and Spellerberg, 2014). However, nowadays they are considered as opportunistic pathogens (Pilarczyk-Zurek et al., 2022). *S. anginosus* is identified in patients suffering from severe infections including bacteraemia, soft tissue abscess, nervous system diseases, and diabetes mellitus (Jiang et al., 2020). A recent report documented that *S. anginosus* promotes gastric inflammation, atrophy, and tumorigenesis (Fu et al., 2024). Of note, *S. anginosus* constitutes an important component of polymicrobial infections in patients with oral, head, neck, and abdominal abscesses, including severe purulent infections with poor outcomes (Al Majid et al., 2020; Furuichi and Horikoshi, 2018; Noguchi et al., 2015; Junckerstorff et al., 2014). Among bacterial pathogens that accompany *S. anginosus* in purulent infections are Gram-positive cocci and Gram-negative bacilli, both aerobic and anaerobic species (Al Majid et al., 2020; Furuichi and Horikoshi, 2018), including *Staphylococcus aureus* (Junckerstorff et al., 2014; Speziale and Pietrocola, 2021), *Klebsiella pneumoniae* (Lau et al., 2007; Shinzato and Saito, 1995; Noguchi et al., 2021), *Pseudomonas aeruginosa* (Cherny and Sauer, 2019; Whiley et al., 2014), *Haemophilus influenzae* (Noguchi et al., 2015; von Köckritz-Blickwede et al., 2016), *Salmonella typhimurium*

* Corresponding author.
E-mail address: joanna.koziel@uj.edu.pl (J. Koziel).
[1] ORCID 0000-0001-6505-3494
[2] ORCID 0000-0003-1925-4011
[3] ORCID 0000-0002-3846-7234
[4] ORCID 0000-0001-6949-4860
[5] ORCID 0000-0002-6571-6259
[6] ORCID 0000-0001-8228-9917
[7] ORCID 0000-0002-3452-8167
[8] ORCID 0000-0003-3436-6425

https://doi.org/10.1016/j.micres.2024.127959
Received 30 August 2024; Received in revised form 18 October 2024; Accepted 29 October 2024
Available online 30 October 2024

(Mónaco et al., 2021), and *Escherichia coli* (Noguchi et al., 2015; von Köckritz-Blickwede et al., 2016; Garcia Gonzalez and Hernandez, 2022; Brinkmann et al., 2004). Despite the emergence of alarming clinical reports, little is known about the virulence factors (VFs) of *S. anginosus*. Finding and characterizing SAGs VFs is an important step in understanding the molecular mechanisms involved in the development of purulent and polybacterial infections caused by *S. anginosus*.

Clinical observations indicate that *S. anginosus* isolates are often associated with soft tissue abscesses (Asam and Spellerberg, 2014). The abscesses are characterized by continuous infiltration of neutrophils and their formation indicates a lack of capacity of these cells to eliminate the pathogen. The evolved protective mechanism of *S. anginosus* against leukocytes was documented *in vitro* and *in vivo* (Budziaszek et al., 2023; Wanahita et al., 2002). It was shown that despite the efficient accumulation of neutrophils at the infection site, *S. anginosus* remains resistant to eradication by those phagocytes. However, the molecular mechanism of the above phenomenon remains unexplained.

The formation of neutrophil extracellular traps (NETs) is one of the main antibacterial mechanisms induced in response to invaders (Garcia Gonzalez and Hernandez, 2022). Those three-dimensional structures are composed of chromatin decorated with antibacterial components released from azurophilic granules of neutrophils (Yang et al., 2016). NETs efficiently entrapped microorganisms limiting their spread, however, many pathogens evolved the mechanism to inactivate the bactericidal activity (Liao et al., 2022). Among them is a modification of the cell wall or secretion of enzymes including DNases (Ríos-López et al., 2021) and proteases (Bryzek et al., 2019), which effectively digest the main components of NETs. These mechanisms were described in detail for other streptococci, including *S. pneumoniae*, *S. pyogenes,* and *S. agalactiae* (Sharma et al., 2019; Sitkiewicz, 2018); however, they have not been studied for *S. anginosus*.

Therefore, we aimed to analyse the interaction of *S. anginosus* with human polymorphonuclear leukocytes with an emphasis on NETs. Using the set of clinical strains, we showed for the first time that *S. anginosus* is a potent NETs inducer, albeit resistant to the antibacterial activity of those structures that depends on the expression of a cell wall-anchored nuclease SanA (*Streptococcus anginosus* Group nuclease A). Moreover, *S. anginosus* avoids its own elimination but also supports the survival of highly pathogenic species from *Enterobacteriales*, protecting them from destruction by neutrophils. Obtained data revealed for the first time that nucleases should be classified among critical *S. anginosus* virulence factors determining severe purulent monospecies infections but also polymicrobial diseases.

2. Results

2.1. Nuclease activity of S. anginosus

Using the collection of clinical *S. anginosus* isolates (n=44) we examined their DNase activity. For this purpose, we applied both qualitative and quantitative methods to study the DNase activity of bacterial culture supernatant and whole bacterial cultures. The degradation of DNA was observed already after 3 hours and progressed after another 24 hours of DNA incubation with bacterial cultures (Fig. 1A, B). Notably, we found no DNase activity in the culture supernatant (data not shown). The observation indicates the presence of DNases anchored to the bacterial cell surface rather than released into the culture medium. The obtained data demonstrated meaningful differences in DNase activity among strains measured after 24 h showing those characterized by low (n=18; e.g. 2218/00, 4393/12), medium (n=9; e.g. 2027/08, 1834/01), or high DNase activity (n=17; e.g. 3792/10, 4695/08) (Fig. 1B, C). Moreover, the dynamics of DNase activity produced by clinical SAG differs among strains thus some high DNase isolates can be defined as “early” (e.g. 3792/10, 884/14, 4695/08) and “late” (e.g. 8328/10, 4020/05, 910/08) producers based on DNase activity measured after 3 and 24 hours (Fig. 1A, B). Additionally, the analysis of clinical data (Budziaszek et al., 2023) revealed that among *S. anginosus* strains with high DNase activity, more than half (56 %, n=9) were isolated from severe infections in contrast to strains with medium and low activity of nucleases (Fig. 1D).

2.2. Nuclease expressed by S. anginosus

To identify *S. anginosus* nuclease/s important in NETs degradation, we selected strains characterized by high (e.g. 3792/10, 4695/08) and low/medium (e.g. 1834/01, 2721/07) activity of DNases (Fig. 1B) and performed genetic analyses which included a search for genes coding for potential DNA degrading enzymes. Such nucleases should be secreted, cell wall-anchored proteins. Therefore, we looked for putative proteins with N-terminal signal sequences, with the sortase recognition signal comprising the LPXTG amino acid sequence within the C-terminus. Genomic analysis revealed a single putative sequence encoding cell wall-anchored nuclease (Suppl. Fig. 1), 736 aa in size, annotated as 5’-nucleotidase. The central domain (pos. 362–667 aa – Fig. 2A) shared sequence similarity with MnuA, a DNaseI-like nuclease of *Mycoplasma pulmonis*. The homologs of this gene and the resulting protein were found only in the SAG members, with *S. anginosus* as the most and *S. intermedius* as the least identical hits analysed at the nucleotide (91–97 % coverage with ca. 84–97 % identity) and protein level (99–100 % coverage, 85.3–99.05 % identity), respectively (Suppl. Table I and II) (Fig. 2C). The gene coding for 736-aa nuclease was detected in genomes of strains with high DNase activity (3792/10, 4695/08, and 980/01) but also in the genomes of the strains characterized by low/medium DNase activity (2721/07, 1834/01) (Suppl. Fig. 1). Alignment of genes coding for the nuclease from all five selected strains revealed that its sequences from 3792/10 and 4695/08 strains cluster with the nucleotide sequences from the same *S. anginosus* strains, while the nuclease genes from 980/01, and 2721/07 group with sequences of other *S. anginosus* strains. Moreover, the nuclease gene from 1834/01 clusters with the *S. constellatus* nuclease gene (Suppl Fig. 2).

To explain the observed difference in nucleolytic activity among strains (Fig. 1A, B) we analysed the expression of this newly identified nuclease, namely SanA (*Streptococcus anginosus* Group nuclease A). The obtained results showed a higher level of mRNA encoding the enzyme in strains with potent nuclease activity (Fig. 2B). Those data clearly indicate that the presence of the gene is not sufficient to ensure high nuclease activity of *S. anginosus*. Moreover, we found that the efficiency of SanA towards nucleic acids increases in the presence of bivalent ions Ca^{2+} and Mg^{2+} (Fig. 2D) and is inhibited by ions chelators (Fig. 2D), which corroborates with the presence of putative Mg binding sites identified in the putative protein sequence (Fig. 2A). The multiple amino acid sequence alignment of SanA of *S. anginosus* 980/01, 3792/10, 4695/08, 2121/07, and 1834/01 strains is presented in supplementary material (Suppl. Fig. 1).

2.3. S. anginosus induces NETs formation with subsequent nuclease-dependent chromatin degradation

The majority of analysed strains with high DNase activity were isolated from severe purulent infections (Fig. 1D) in which accumulation of neutrophils and enhanced formation of NETs is observed. The above suggests the role of nucleases as virulence factors of *S. anginosus* that modulate the function of neutrophils. Therefore, we decided to assess whether the level of SanA could play a role in the regulation of NETs. For the tests of NETs regulation, we selected two strains with high (3792/10, 4695/08) and low/medium (1834/01, 2721/07) DNase activity (Fig. 1B). It was also important for us to select those strains that efficiently degrade DNA after a short period of time, within 3 h, as during this time the bacteria can be inactivated by NETs. This is crucial in the assumption that to avoid killing by NETs, bacteria must efficiently break free from the chromatin network. We determined that all selected strains induce the release of DNA (Fig. 3A) and formation of NETs by

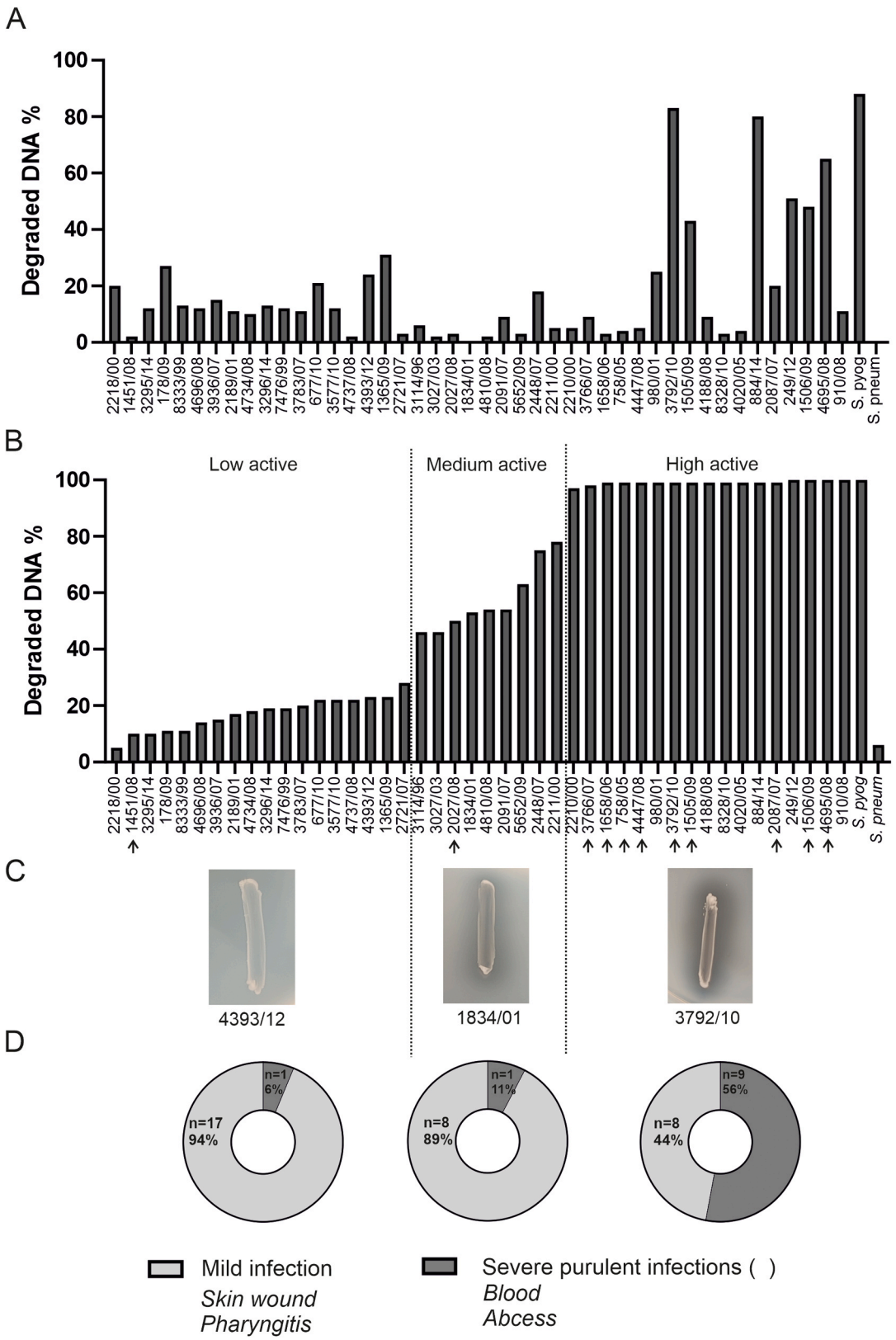

Fig. 1. The Assessment of DNase activity produced by *S. anginosus* clinical strains. (A, B) The quantitative eukaryotic DNA degradation displaying differential DNase activity between *S. anginosus* strains. Whole bacterial cultures were incubated with salmon sperm DNA for 3 h and 24 h. Fluorescent SYBR Green dye was used to quantify the remaining dsDNA. The bar graph presents the percentage of degraded DNA. *S. pyogenes* strain served as a positive control as it is a potent DNA degrader, *S. pneumoniae* strain served as a negative control as it does not degrade external DNA. The arrows indicate *S. anginosus* isolated from purulent infections; (C) In the qualitative estimation of DNase activity, *S. anginosus* strains were grown on BD DNase Test Agar; (D) Percent of strains isolated from severe purulent infection in groups of low, medium, and high DNase activity.

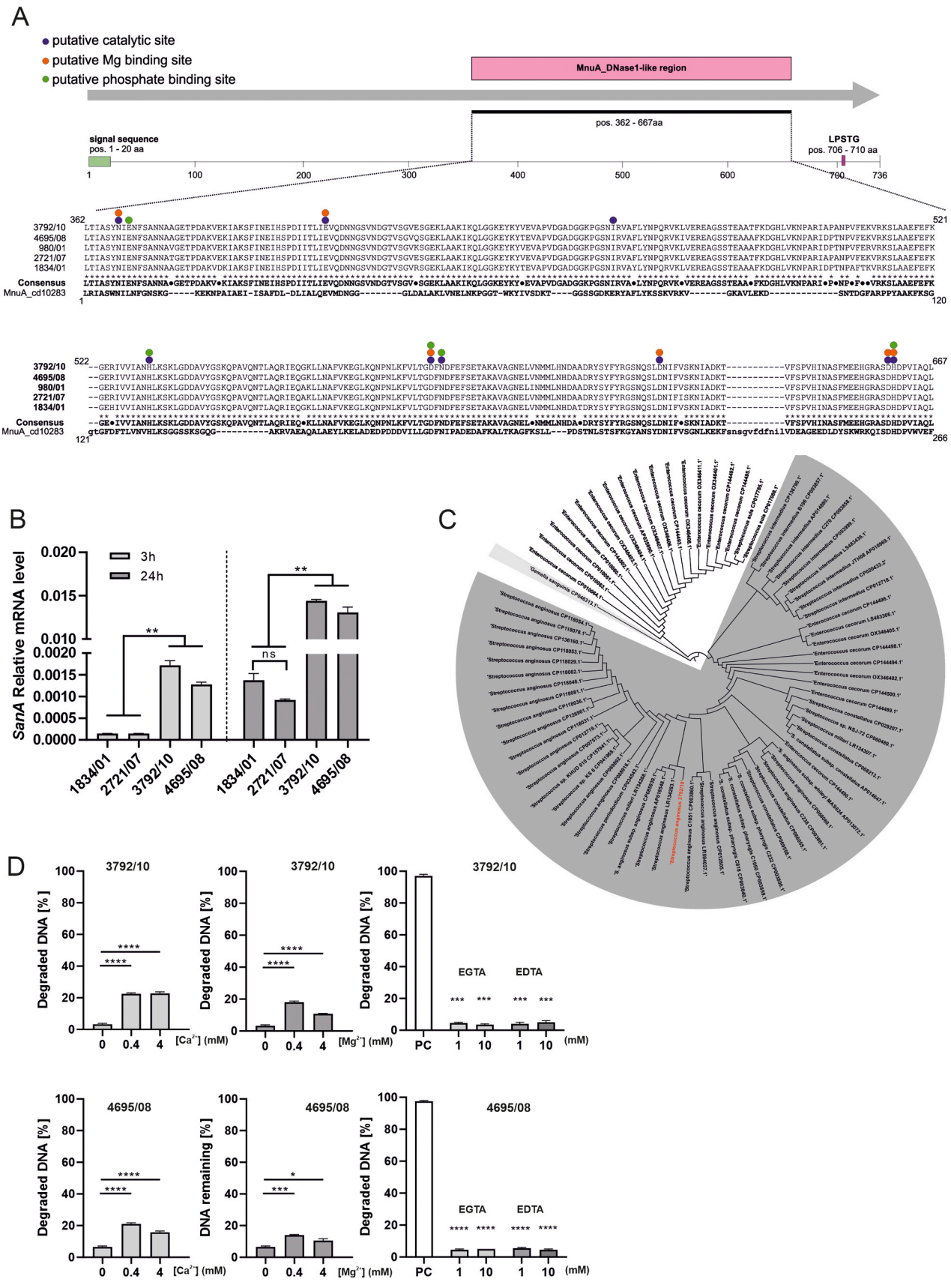

(caption on next page)

Fig. 2. The nuclease expressed by *S. anginosus*. (A) A translated nucleotide sequence analysis of selected *S. anginosus* strains revealed a single putative sequence encoding cell wall-anchored protein namely SanA. The protein is 736 aa in size and shares homology with 5'-nucleotidase nuclease; (B) qRT-PCR analysis of nuclease *sanA* gene expression level. RNA from bacteria with high (3792/10, 4695/08) and low (1834/01, 2721/07) nucleolytic activity collected from logarithmic (3 h) and stationary phase growth (6 h). Relative expression was performed using qRT-PCR with *tufA* used for normalization of quantification; (C) Neighbour-joining phylogenetic tree of *sanA* of *S. anginosus* 3792/10. The tree was calculated using BlastN pairwise alignment with the NCBI's New BLAST Core Nucleotide Database. The iTol tool (https://itol.embl.de/) was used for the tree visualization. In red - *sanA* of *S. anginosus* 3792/10 used as a query. The sequences with 91–100 % query coverage are shaded in dark gray, those with 52 % in light gray, and those with 2 % are not shaded; (D) Analysis of the effect of the presence Ca^{2+} and Mg^{2+} and ion chelators EDTA and EGTA on DNase activity by SYBR Green assay. The reaction was performed in 40 mM HEPES (pH=7.5) in the absence or presence of 0.4 or 4.0 mM Ca^{2+} and Mg^{2+}. Positive control (PC) consisted of DNA in DNase buffer with bacteria. Data represent mean values from three independent experiments ± SEM. P values indicated by *, P, 0.05; **, P, 0.01; ***, P, 0.001; ****, P, 0.0001.

neutrophils showing the structures of chromatin decorated with elastase (Fig. 3B). The number of netting neutrophils was comparable among strains (Fig. 3C). Importantly, despite initially high production of NETs, we found the significant reduction of their length 3 hours after infection of neutrophils with high activity DNase strains (Fig. 3D, E) indicating the degradation of NETs by nucleases.

2.4. Survival of S. anginosus in NETs depends on DNase expression

To assess the antibacterial activity of NETs towards *S. anginosus*, selected strains were co-incubated with neutrophils pretreated with or without Cytochalasin D (CytD). Application of cytochalasin D is usually used to distinguish between phagocytic and NET microbicidal activity (Buchanan et al., 2006). Further, selected strains were co-incubated with neutrophils with or without micrococcal nuclease (MNase) to detach NETs from cell fragments (Meijer et al., 2012). Bacterial survival was analysed by counting colony-forming units (CFU) (Fig. 4A). We observed that *S. anginosus* strains with low/medium DNase activity (1834/01, 2721/07) were effectively killed by NETs in contrast to strains with high nuclease activity (3792/10, 4695/08) (Fig. 4A). To confirm the inactivation of NETs by *S. anginosus* nuclease, PMA-derived NETs were exposed to *S. anginosus* with following survival rate detection (Fig. 4B). Our results confirmed that PMA-generated NETs did not affect the viability of DNase-rich strains (3792/10, 4695/08), but markedly reduced the survival of *S. anginosus* strains with low expression of the enzyme (1834/01, 2721/07) (Fig. 4B). Additionally, external DNase limited the bactericidal activity of NETs against low/medium DNase strains (Fig. 4B), highlighting the crucial role of *S. anginosus* DNase in the protection against NETs. Bacterial viability using LIVE/DEAD staining revealed entrapped and non-viable bacteria only in the case of strains (1834/01, 2721/07) with low levels of nuclease (Fig. 4C). In order to confirm the role of DNase in the resistance of *S. anginosus* to NETs we constructed mutants of *S. anginosus* 3792/10 strain devoid of DNase expression (Suppl. Fig. 3). To identify the DNase important in NETs digestion the transposon mutagenesis of the *S. anginosus* 3792/10 strain was performed followed by selection of mutants deficient in external DNA degradation. The pGh9:IS*S1* plasmid with a thermo-sensitive origin of replication, conferring erythromycin (Ery) resistance was used as the donor of the IS*S1* transposon (Maguin et al., 1996). At a non-permissive temperature (38°C) Ery-resistant clones were selected and then tested for DNase production. Of over 7700 clones, three were regarded as DNase-negative. The IS*S1* integration sites in those three independently selected DNase-deficient *S. anginosus* 3792/10 mutants were determined and pointed to the single gene (*sanA*) coding for 736-aa nuclease detected previously *in silico*. The genome of *S. anginosus* 3791/10 *sanA*::IS*S1* insertion mutant was sequenced to obtain its complete structure and to verify the IS*S1* integration site. As a result, the single integration site of pGh9:IS*S1* was detected, located within the *sanA* gene.

The lack of SanA does not influence the generation time (Fig. 4D), whereas significantly reduces DNase expression (Fig. 4E) and activity (Fig. 4F). We found efficient eradication of mutant *S. anginosus* 3792/10 *sanA*::IS*S1* when compared to WT by NETs using LIVE/DEAD staining (Fig. 4G) and CFU plating method (Fig. 4H). Collectively, our findings demonstrate that SanA DNase activity is a crucial factor determining the survival of *S. anginosus* in the NETs environment.

2.5. Inactivation of NETs by nucleases promotes systemic infection with S. anginosus

To examine the role of nucleases in the inactivation of NETs *in vivo* we applied the model of *Galleria mellonella* infection (Budziaszek et al., 2023). The innate immune response of larvae shows similarities to the immune response in vertebrates and nucleic acids released from hemocytes are thought to play a comparable role to NETs by trapping and killing pathogens (Browne et al., 2013). The larvae were infected with the WT strain of *S. anginosus* (3792/10) and its isogenic DNase-deficient mutant (*sanA*::IS*S1*). The infection of larvae with the WT strain resulted in 100 % mortality 24 h post-infection (p.i.) at a dose of 1×10^7 CFU/larva (Fig. 5A), whereas we found a significant extension of the larvae survival after infection with the DNase deficient strain (*S. anginosus* 3792/10 *sanA*::IS*S1*). Moreover, we observed more severe symptoms in *G. mellonella* infected with *S. anginosus* WT than in those infected with the *sanA*::IS*S1* mutant (Fig. 5B). We showed that systemic distribution and proliferation of bacteria were diminished in larvae infected with strains with nuclease deficiency (Fig. 5C) what might be explained by efficient trapping and killing of nuclease deficient strain by NETs forming by activated hemocytes (Fig. 5D). Presented difference in the virulence *in vivo* between the wild-type strain and the strain DNase-deficient, indicates that SanA DNase plays a critical role in *S. anginosus* pathogenicity.

2.6. S. anginosus protects accompanying pathogens against elimination by NETs

S. anginosus is often identified in multispecies infections (Al Majid et al., 2020; Furuichi and Horikoshi, 2018; Noguchi et al., 2015, 2021), so it is likely that inactivation of NETs will promote the survival of other coexisting bacterial species. Microorganisms accompanying *S. anginosus* differ in term of nuclease expression, subcellular localization of enzymes, and susceptibility to elimination by NETs (Fig. 6A) (Junckerstorff et al., 2014; Speziale and Pietrocola, 2021; von Köckritz-Blickwede et al., 2016; Garcia Gonzalez and Hernandez, 2022; Derré-Bobillot et al., 2013; Ajit et al., 2023; Mücke et al., 2017; Wilton et al., 2018; Juneau et al., 2015; Doke et al., 2017). To verify our hypothesis we selected bacteria clinically associated with *S. anginosus*, which do not express secreted nucleases and are sensitive to the bactericidal activity of NETs: *Escherichia coli (E.c.), Salmonella enterica (S.e.), Klebsiella pneumoniae (K. p.),* and *Enterococcus faecalis (E.f.)* (Fig. 6A) (Mónaco et al., 2021; Garcia Gonzalez and Hernandez, 2022; Brinkmann et al., 2004). We confirmed no extracellular nuclease activity for all selected bacterial strains (*E.c, S. e, K.p, E.f*) (Suppl. Fig. 4). We found that *S. anginosus* does not affect the growth of the tested species (Fig. 6B). We also confirmed the susceptibility of selected bacteria to PMA-derived NET (Fig. 6C). Then, we determined that the presence of *S. anginosus* strain 3792/10 efficiently protects pathogenic *Enterobacteriales* species and *E. faecalis* against killing by NETs (Fig. 6D). The effect was observed for multiple species already at the ratio of 1:5 of the pathogen to *S. anginosus* (Fig. 6D). Obtained results (Fig. 6D) can be explained by decreased efficiency of pathogens entrapment in the chromatin network (Fig. 6E). This

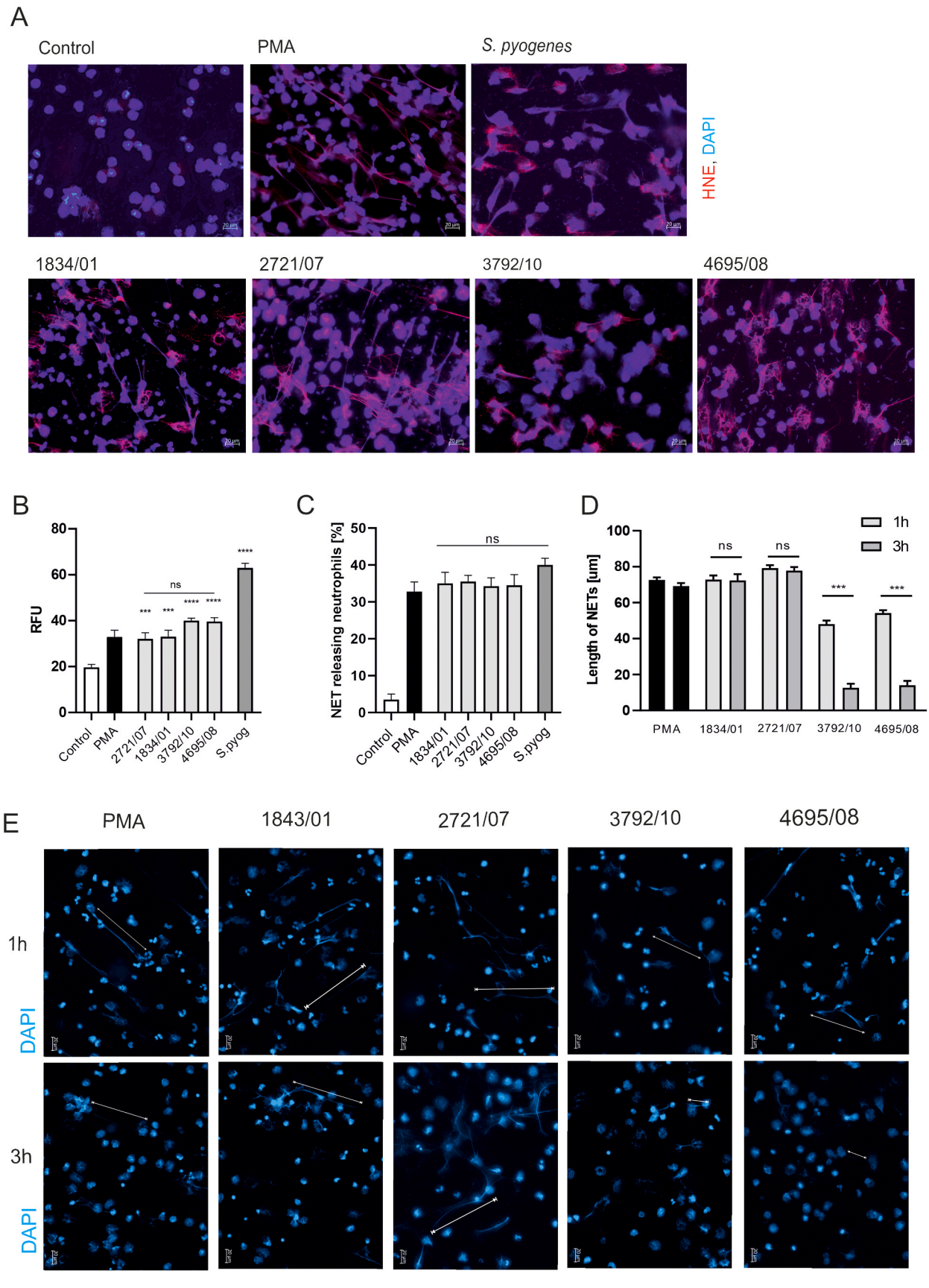

(caption on next page)

Fig. 3. The generation of NETs by *S. anginosus*. (A) Formation of NETs by *S. anginosus* strains with high (3792/10, 4695/08) and low (1834/01, 2721/07) nucleolytic activity. As a positive control, PMA (25 nM) stimulation was applied. *S. pyogenes* was used as a reference strain. The level of extracellular DNA released by human neutrophils 1 h post-bacterial exposure at MOI 1:5 was estimated by Quantitative PicoGreen (QPG). Mean data (± SEM) from 3 independent experiments are shown. (B) Visualization of NETs by fluorescent microscopy. DNA is shown in blue (DAPI) and human neutrophil elastase (HNE) is shown in red. Bars represent 20 μm; (C) Quantitative analysis of NETs images was performed by counting the number of neutrophils releasing NETs from 12 different fields of view. The results are presented as a mean value (± SEM); (D, E) The reduction of *S. anginosus*-derived NETs in relation to the nuclease activity of tested strains after 1 h and 3 h post infection. DNA is shown in blue (DAPI), and white arrows show length of individual NET. Bars represent 20 μm. Mean data (± SEM) from 3 independent experiments using neutrophils from different healthy donors are shown. P values indicated by *, P, 0.05; **, P, 0.01; ***, P, 0.001; ****, P, 0.0001; ns, non-significant.

phenomenon can be confirmed *in vivo* as we observed a significant increase of *E. coli* growth during the coinfection with *S. anginosus* (Fig. 6F). Moreover, we showed that SanA is responsible for the observed protection of *E. coli* strain belongs to *Enterobacteriales* against NETs (Fig. 6G). Collectively, we presented for the first time that the SanA nuclease of *S. anginosus* supports not only SAG pathogenicity but also protects *Enterobacterales* and other pathogenic microorganisms against elimination by NETs.

2.7. Discussion

The molecular basis of *S. anginosus* pathogenesis remains elusive, as does its role in polymicrobial diseases (Asam and Spellerberg, 2014). It is highly likely that the virulence of this species is based on molecular mechanisms similar to those of other streptococci. Among these are capsule formation (Cumley et al., 2012), expression of adhesins (Schüler et al., 2012), and hyaluronidases (Wang et al., 2014). It was also reported that nuclease activity should be considered as a virulence factor (Jacobs and Stobberingh, 1995). The latter, SanA nuclease, is important for the neutralization of neutrophil extracellular traps. In this respect, *S. anginosus* is similar to other streptococci that express either surface-exposed or secreted nucleases, which contribute to bacterial survival when trapped in NETs.

Several species of *Streptococcus* produce nucleases which degrade the DNA backbone of NETs, reducing the effectiveness of NETs and resulting in increased pathogenicity (Liao et al., 2022). It has been shown that Group A *Streptococcus* (GAS) produce 26–30 nucleases, among which Sda1 and SdaD2 play the most important roles in virulence (Sumby et al., 2005). *Streptococcus pyogenes* nuclease A (SpnA) is a cell wall-anchored nuclease that is able to digest chromatin in NETs (Chang et al., 2011). Surface-exposed nucleases with a confirmed role in virulence have also been described in other pathogenic streptococcal species, such as EndA from *Streptococcus pneumoniae*, Nuclease A from *Streptococcus agalactiae* (Group B Streptococcus), streptococcal wall-anchored nuclease (SWAN) from *Streptococcus sanguinis*, and SsnA from *Streptococcus suis* (Chalmers et al., 2020). We have identified for the first time the SanA nuclease. We found that the enzyme is unique to the *S. anginosus* group (SAG) and is encoded by all tested *S. anginosus* strains with high similarity to putative sites of nucleases in *S. intermedius* and *S. constellatus*. Both Ca^{2+} and Mg^{2+} are required for its optimal activity towards eukaryotic DNA. We also found that *sanA* mRNA expression level is strain-dependent, therefore, the regulation mechanism and precise identification of substrate specificity are needed. High heterogeneity in terms of SanA nuclease activity among strains correlates with their effectiveness against NETs and the severity of clinical signs of infection. Strains isolated from severe, purulent infections, including abscesses which are the consequence of bacteraemia, showed higher DNase activity compared to strains isolated from mild infections. Therefore, hereby we postulate the important role of SanA nuclease in the pathogenesis of *S. anginosus*. Abscess formation is characterized by the accumulation of leukocytes attempting to eliminate the invaders, which may indicate an insufficient ability of neutrophils to eliminate *S. anginosus*. Our research indicates that SanA nuclease is among the factors that paralyse the antibacterial activity of neutrophils, contributing to the virulence of invasive *S. anginosus* strains by allowing the bacteria to escape NET-mediated killing (Buchanan et al., 2006). We show that strains characterized by high DNase activity can survive better in the presence of neutrophils compared to strains that produce lower levels of SanA. We also demonstrated SanA nuclease as a critical factor that ensures the survival of *S. anginosus* in the presence of NETs in a simplified *in vivo* model, showing that deletion of *sanA* resulted in a lower bacterial burden and delayed death of wax worms. The obtained data suggest that SanA is required for full virulence, which could be confirmed in a more advanced infection model in the future, such as mice infection of human *ex vivo* models. The role of SanA during human infection remains to be further elucidated, taking into consideration that *S. anginosus* can be highly pathogenic under predisposing conditions, especially in immunocompromised patients (Al Majid et al., 2020). Besides inactivation of NETs it would be valuable to specify the role of SanA in biofilm formation and the regulation of the host response to nucleic acids.

The above observations may explain the development of acute and chronic *S. anginosus* infections, as well as the cause of multispecies infections in which streptococci are identified. Co-infections of SAG with other microorganisms have been observed in many clinical studies (Noguchi et al., 2015, 2021; Mücke et al., 2017). Anaerobes of oral origin, particularly from the genera *Peptostreptococcus, Prevotella,* or *Fusobacterium*, mixed with SAG, were frequently isolated from pulmonary infections (Shinzato and Saito, 1995). For example, it was shown that SAG in combination with *P. intermedia* caused more severe pneumonia and higher mortality in mice. Moreover, animals infected with the microbial combination also developed lung abscesses or empyema. These experiments demonstrate clinically important role of *S. anginosus* in mixed infections (Noguchi et al., 2015; Shinzato and Saito, 1994). The mechanisms of synergy between certain aerobes and anaerobes have been already suggested. One of the most important include (i) the production of various growth factors by the bacteria during co-infection; (ii) the ability of anaerobes to inhibit phagocytosis of aerobes by leukocytes; (iii) alteration of the local environment, including reduction of oxygen tension and lowering of the redox potential; and (iv) the production of substances toxic to the host (Shinzato and Saito, 1994). However, so far, no mechanism has been proposed to support the survival and growth of bacteria protected by DNase produced by other bacterial species. In our work, we point out that pathogenic bacteria from *Enterobacteriales* and *E. faecalis* accompanying *S. anginosus* are shielded from the antibacterial activity of NETs by SanA activity. Research on the production of DNases as *S. anginosus* virulence factors will significantly expand our basic knowledge but will also allow for the design of drugs that neutralize nuclease activity in order to maintain the integrity of the host's NETs and the ability to effectively combat pathogenic microorganisms. Additionally, utilizing the catalytic activity of *S. anginosus* nucleases offers new possibilities for use as a biomarker of infection (Garcia Gonzalez and Hernandez, 2022).

Collectively, in our studies, we show for the first time that the virulence strategy of *S. anginosus* involves the inactivation of NETs. The degradation of chromatin fibers and the escape of streptococci can be considered as the adaptation of commensals to the host defense mechanisms. Consequently, *S. anginosus* bacteria are not eradicated and can efficiently protect the host. However, in the presence of other pathogens, *S. anginosus* may have a harmful effect by promoting the growth of pathogenic microorganisms. Therefore, we propose that *S. anginosus* should be classified as an opportunistic pathogen that corroborates the immune system to control its own fitness. On the other hand, it facilitates infections with other bacterial species, potentially contributing to

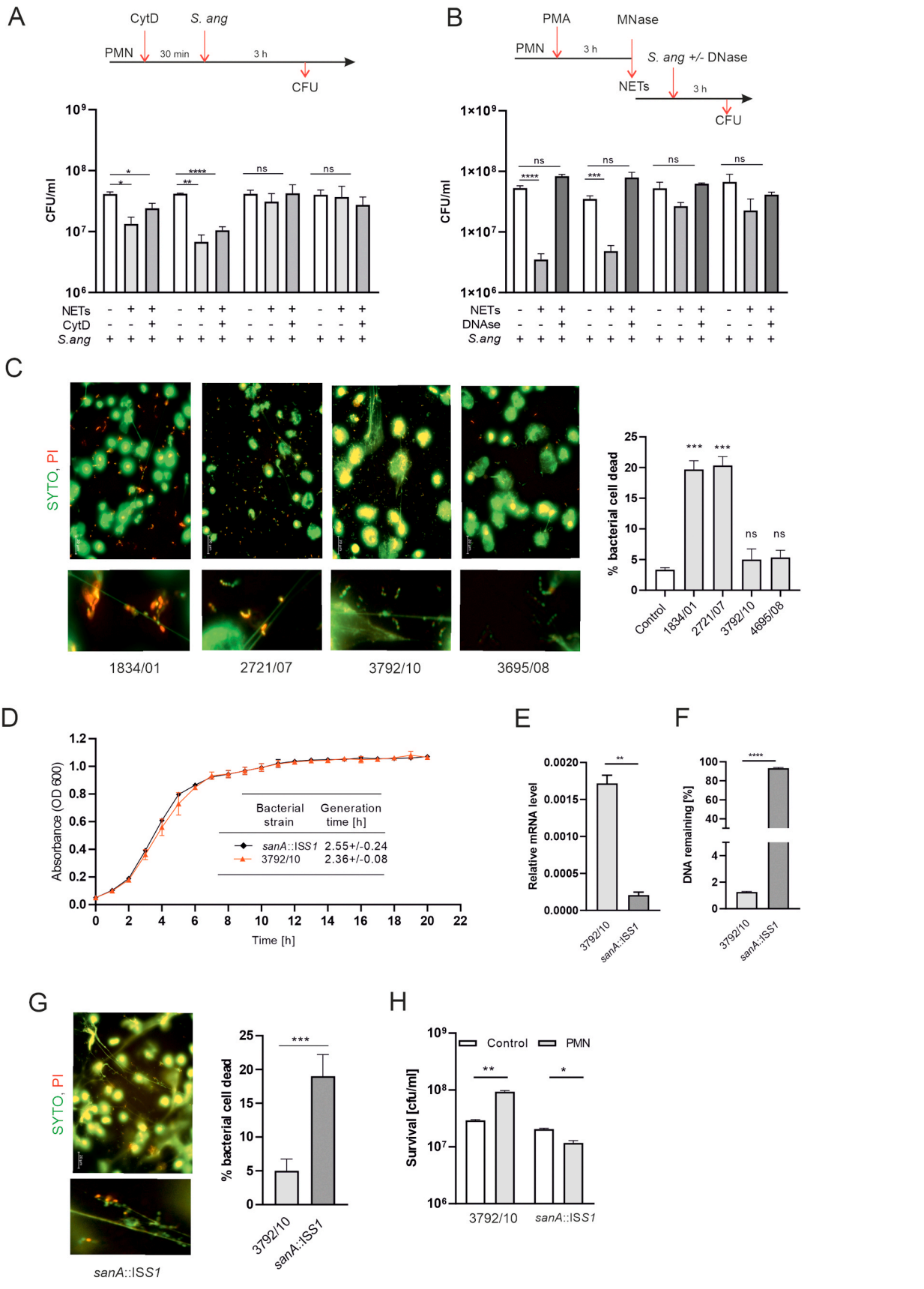

(caption on next page)

Fig. 4. Entrapment and survival of *S. anginosus* in NETs. (A) Survival of *S. anginosus* strains in the presence of PMNs and/or PMNs treated with Cytochalasin D at MOI 1:5; (B) Survival of *S. anginosus* by PMA-derived NETs in the presence of DNase at MOI 1:5; (C) *S. anginosus* entrapment and survival in PMA-derived NETs determined by LIVE/DEAD staining. Viable cells of *S. anginosus* are stained green (SYTO 9), while red signal (Propidium iodide) represents dead bacteria. The scale bar represents 20 μm. Quantitative analysis of dead bacteria to total number of bacterial cells was performed using 6 different fields of view; (D) Growth curve of *S. anginosus* 3792/10 and *sanA*::IS*S1* strains in TSB at 37°C, 5 % CO_2. (E) Comparison of DNase gene expression in WT and isogenic *sanA*::IS*S1* strain by qRT-PCR; (F) Determination of DNase activity of *sanA*::IS*S1* strain using quantitative DNA assay; (G, H) The survival of *S. anginosus* WT and isogenic *sanA*::IS*S1* strain determined by (G) *S. anginosus* survival in PMA-derived NETs determined by LIVE/DEAD staining and (H) CFU counting. Bacteria were added to NETs or medium after 2 h of incubation bacteria were plated and CFU were determined. Scale bar represents 20 μm. Mean data (± SEM) from 3 independent experiments using neutrophils from different healthy donors are shown. P values indicated by *, P, 0.05; **, P, 0.01; ***, P, 0.001; ****, P, 0.0001; ns, non-significant.

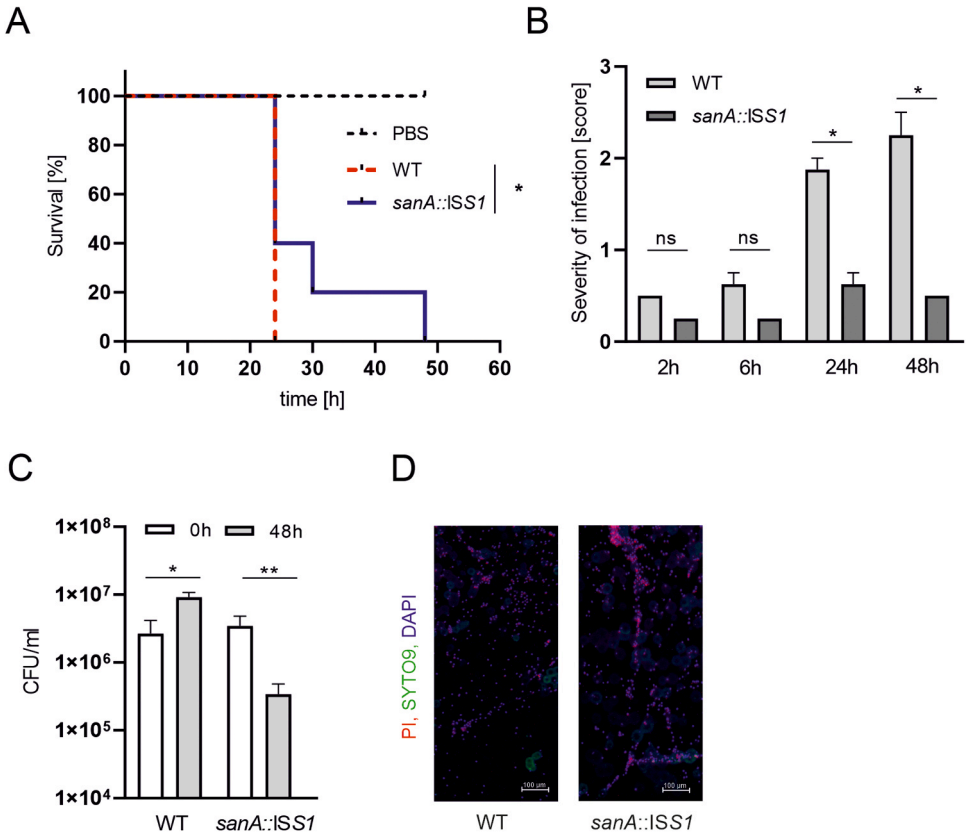

Fig. 5. Attenuation of SanA deficient strain *in vivo* using *G. mellonella* larvae model. (A) Kaplan-Meier survival curves after infection of *G. mellonella* with 10^7 CFU/larva of *S. anginosus* cells; (B) health index scores of *G. mellonella* larvae after infection with 10^6 CFU/larva of *S. anginosus* WT or *sanA*::IS*S1*. The control group was injected with PBS. Each tested group contained 10 larvae (n = 10); (C) survival of *S. anginosus* strains in *G. mellonella* infected 10^6 per larvae; (D) WT and *sanA*::IS*S1* mutant stained with LIVE/DEAD BacLight kit and entrapped in extracellular DNA (DAPI blue fluorescence) released by *G. mellonella* hemocytes after 24 h coincubation with *sanA*::IS*S1* 10^6 per larvae. Scale bars: 100 μm. In all panels that include error bars, the data represent the mean values ± SEM. *P < 0.05; ns, non-significant.

the development of polymicrobial diseases.

3. Materials and methods

3.1. Bacterial strains and cultures

S. anginosus strains were obtained from the National Medicines Institute, Warsaw, Poland (Obszańska et al., 2016), while the *Streptococcus pneumoniae* 49619 and *Streptococcus pyogenes* AA-595 was purchased from ATCC. *Salmonella enterica subsp. enterica* ATCC 14028, *Klebsiella pneumoniae* ATCC 13883, *Enterococcus faecalis* ATCC 29212, and *Escherichia coli* ATCC 25922 were purchased commercially. *Streptococcus* sp. strains were cultured on Columbia Agar (Sigma-Aldrich) with 5 % sheep blood at 37°C with 5 % CO_2. *Enterobacteriales* were grown on McConkey Agar (Sigma-Aldrich). Bacteria were grown in Tryptic Soy Broth (TSB, Sigma-Aldrich) a liquid medium at 37°C with 5 % CO_2. Bacterial cells were collected by centrifugation after overnight culture (5000 × g for 5 min at 20°C), washed twice with PBS, and resuspended in PBS to an optical density of 1.0 measured at 600 nm (OD600), which corresponds to 1×10^8 CFU per ml (CFU/ml).

3.2. Sequencing and analysis of nuclease genes

Sequencing of *S. anginosus* genomes, the potential nuclease producers was performed in the Illumina technique by the DNA Sequencing and Synthesis Facility, IBB PAS (manuscript in preparation). The structure of pGh9::IS*S1* insertion in the *S. anginosus* 3792/10 *sanA*::IS*S1* strain was confirmed by the long-read sequencing of its genomic DNA using Oxford Nanopore technology to obtain complete physical structure (the DNA Sequencing and Synthesis Facility, IBB PAS). SignalP 6.0 (Teufel et al., 2022) was used to detect the N-terminal signal sequence in putative proteins, and PSORTb 3.0 (Yu et al., 2010) to predict their subcellular localization, including the LPXTG amino acid sequence within the C-terminus. DNA and protein sequences were further analysed with BlastN (Altschul et al., 1990) and BlastP (Camacho et al., 2009), respectively. The phylogenetic tree of SanA of *S. anginosus*

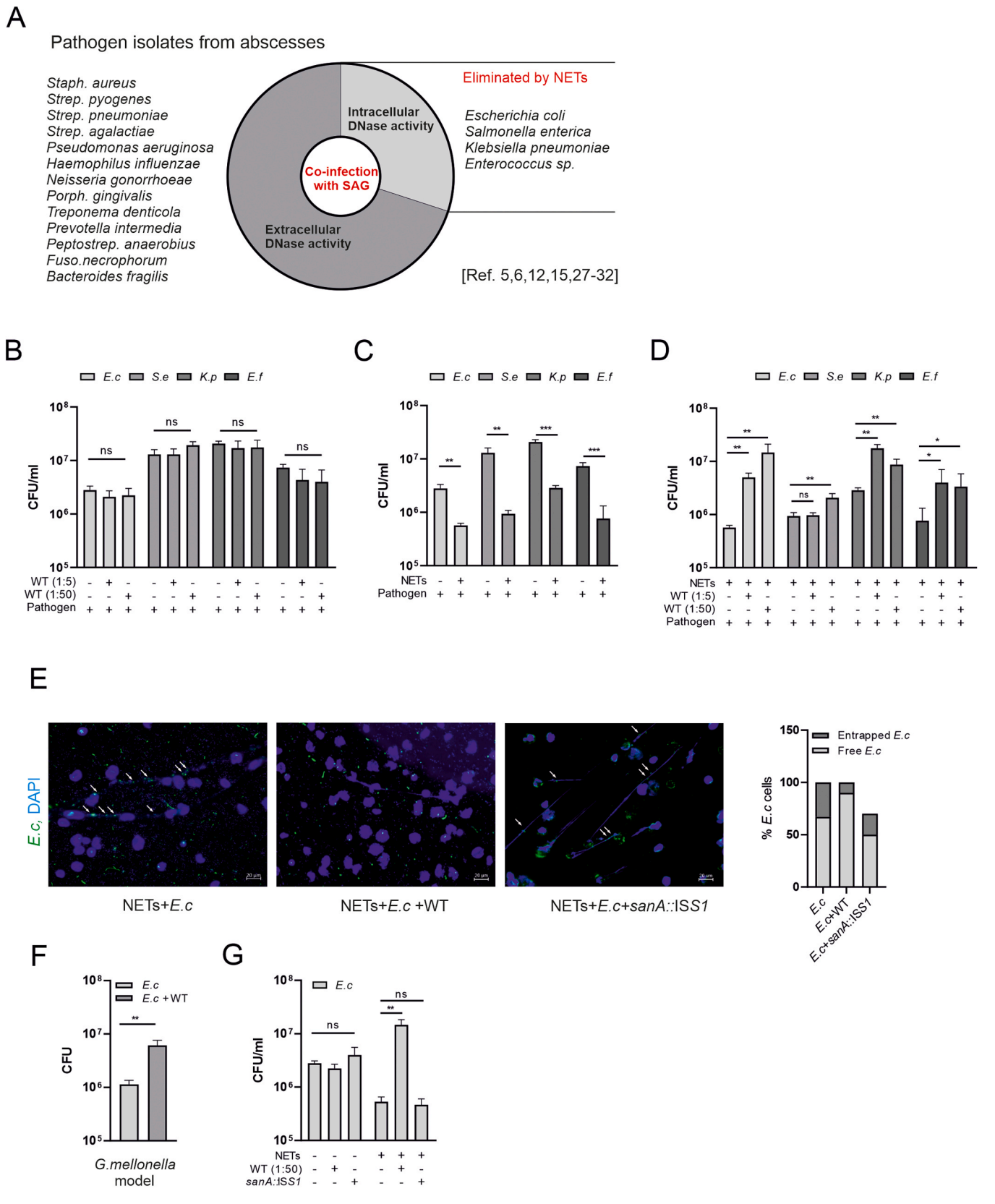

(caption on next page)

Fig. 6. *S. anginosus* activity supports survival of pathogenic species. (A) Pathogens identified in co-infection with *S. anginosus* isolated from abscesses; (B) Growth of pathogens (*E. coli - E.c, Salmonella enterica - S.e, Klebsiella pneumoniae - K.p, Enterococcus faecalis - E.f*) in the presence and/or absence of *S. anginosus* 3792/10 (WT) at ration 1:5 and 1:50; (C) The survival of *Enterobacterales* strains in PMA-derived NETs. Bacteria were added to NETs or medium and after 2 h of incubation were plated and CFU was determined; (D) Survival of *Enterobacterales* strains in PMA-derived NETs in the presence of *S. anginosus* 3792/10 (WT) at the ratio 1:5 and 1:50; *Enterobacterales* strains were added to NETs or medium and after 2 h of incubation were plated on McConkey or Columbia agar and CFU was determined; (E) *E. coli* entrapped by NETs in the presence or without highly active *S. anginosus* WT (3792/10). Neutrophils were activated with PMA for 3 h. Then CSFE-labeled *E. coli* and WT *S. anginosus* strains were mixed in a ratio 1:5 and incubated for 2 h followed by DNA labeling with DAPI. *E. coli* appeared as fluorescent green spots. Bacteria entrapped on the chromatin network are indicated with arrows. Representative image with quantification of entrapped *E. coli* were counted within 4 different fields of view; (F) Survival of *E. coli* in *G. mellonella* model with or without *S. anginosus* coinfection; (G) Survival of *E. coli* in PMA-derived NETs in the presence of *S. anginosus* WT or *sanA*::IS*S1* mutant. Mean data (± SEM) from 3 independent experiments using neutrophils from different healthy donors are shown. P values indicated by *, P, 0.05; **, P, 0.01; ***, P, 0.001; ****, P, 0.0001; ns, non-significant.

3792/10, was calculated with BLASTp (https://blast.ncbi.nlm.nih.gov/Blast.cgi; with fast minimum evolution method and default parameters), and visualised with the iTOL v6.0 tool (https://itol.embl.de) with ignored branches length.

3.3. Growth curve, RNA isolation, and qRT-PCR

Bacteria were inoculated to TSB medium at OD600 of 0.05 in duplicates and grown at 37°C under microaerophilic conditions with 5 % CO_2. The optical density of the culture was measured at 600 nm every 2 h for 24 h. Generation times (G) were calculated with the equation G = 0.301/a, where a is the slope of the linear part of the growth curve. RNA was extracted from bacterial culture from logarithmic (3 h) and stationary (24 h) phases of growth,

Total RNA isolation, reverse transcription, and real-time PCR were performed as described previously (Budziaszek et al., 2023). The sequences of the primers for the detection of nuclease *sanA*: 5′-GATCCCGTCATTGCACAGCTTG-3′, 5′-TCAGCACCTGTTGTTCCTGTAG-3′ product 164 bp, T(melting) 73°C, T(annealing) 50°C and reference gene *tufA*: 5′-CCGTGACCTTCTTTCAGAATAC-3′, 5′-GTCACGTTCTGGTTCTGGAATG-3′ product 157 bp, T(melting) 71°C, T(annealing) 48°C.

3.4. Construction of DNase deficient strains

The transposon mutagenesis was performed to obtain a DNase-deficient mutant in the *S. anginosus* 3792/10 strain (Suppl. Fig. 3). For this purpose, the pGh9:IS*S1* plasmid (Maguin et al., 1996), a carrier of the transposon IS*S1*, with a thermosensitive origin of replication was used. It was introduced to the *S. anginosus* by electroporation as described previously for *Streptococcus agalactiae* (Ricci et al., 1994). Erythromycin (Ery)-resistant clones were selected at 28°C, on BHI agar (Brain Heart Infusion, Oxoid, solidified with 1.5 % agar) supplemented with erythromycin (5 mg/L). The IS*S1* transposition was induced at 38°C as described for *Lactococcus lactis* by Maguin (Maguin et al., 1996). Ery-resistant clones were selected at 38°C. The transposition frequency was 1.9 %, regarded as the number of Ery-resistant cells (counted on BHI agar with Ery at 38°C) divided by the total cell count (measured on BHI medium at 38°C). The Ery-resistant clones were then streaked on DNase Test Agar plates (BD Micro Systems). Clones unable to form clear zones were regarded as DNase-negative. The IS*S1* integration site was determined – the chromosomal DNA was isolated from mutants (Genomic Micro AX Bacteria+ Gravity, A&A Biotechnology, Gdansk, Poland), digested with *Hin*dIII (Thermo Fisher Scientific Inc., USA), self-ligated, amplified with primers 5'-CAAACTGCCTCAACCACGATTAAGG-3' and 5'-CCAGAGATGATAGAGGACTTTAC-3' with the use of Premix Taq™ DNA Polymerase (TaKaRa Taq™ Version 2.0, Takara Bio, Shiga, Japan), and finally sequenced.

3.5. Determination of DNase activity

S. anginosus strains were characterized for DNase activity using a qualitative method with a plate assay. Briefly, plate agar cultures of *S. anginosus* were spotted on the surface of DNase Test Agar plates (BD Micro. Systems) and incubated for 24 h at 37°C. After adding 0.1 M HCl for 3 min, the appearance of a clear zone around bacterial growth indicated DNA degradation. DNase activity of *S. anginosus* was also determined by quantification of residual DNA after incubation of bacterial cells with 100 μg/ml salmon sperm DNA (Sigma-Aldrich) prepared in DNase buffer (5.96 g/L HEPES, 590 mg/L $CaCl_2$*$2H_20$, 380 mg/L $MgCl_2$; pH 7.5 in RNase/DNase-free water). *Streptococcus pyogenes* AA-595 was used as the reference.

Analysis of the effect of the presence Ca^{2+} and Mg^{2+} on DNase activity was also determined. The reaction was performed in 40 mM HEPES (pH=7.5) in absence or presence of 0.4 or 4.0 mM Ca^{2+} and Mg^{2+}. Additionally, ion chelators (ethylenediaminetetraacetic acid [EDTA] and ethylene glycol tetraacetic acid [EGTA]) were tested for inhibition of *S. anginosus* DNase activity at 1 and 10 mM. Following incubation 24 h at 37°C DNA was quantified by adding the SYBR Green reagent. Positive control consisted of DNA in DNase buffer (5.96 g/L HEPES, 590 mg/L $CaCl_2$*$2H_20$, 380 mg/L $MgCl_2$; pH 7.5 in RNase/DNase-free water). Fluorescence was measured with a FlexStation microplate reader at an excitation wavelength of 498 nm and an emission wavelength of 520 nm. The % of degraded DNA which was calculated based on the formula: Degraded DNA [%] = 100 – [(fluorescence of treated sample/fluorescence of only DNA control) x 100 %].

3.6. Isolation of human neutrophils, induction and quantification of NETs

Human blood was purchased from the Regional Blood Centre, Krakow, Poland. Neutrophils were isolated as described before (Bryzek et al., 2019). Neutrophils were seeded at 2×10^6/well in 0.01 mg/ml poly-L-lysine-coated 24-well plates and centrifuged (200 × g, 5 min) to allow cells to adhere to the plates. Then, neutrophils were stimulated at 37°C with the following: PMA 25 nM as a positive control, strains of *S. anginosus* or *S. pyogenes* as a reference, at a multiplicity of infection (MOI) of 1:5 by 1 h or 3 h, 37°C, 5 % CO_2. Next, culture media from untreated (control) or treated neutrophils was collected and the amount of extracellular DNA was quantified using QuantiPicoGreen (QPG) diluted 1:200 in TE buffer (10 mM Tris, 1 mM EDTA; pH 7.5) 90 μl of diluted QPG was mixed with 10 μl of supernatant containing the extracellular DNA. The fluorescence was measured at an excitation wavelength of 480 nm and an emission wavelength of 520 nm. All experiments were performed in biological triplicates using different blood donors each with two or three technical replicates.

3.7. PMN killing assay

A suspension of *S. anginosus* in DMEM (without phenol red) with 1 % human serum was added to 5×10^5 polymorphonuclear leukocytes (PMN)/well seeded in DMEM in 96-well plates at an MOI of 1:5 (cells-to-bacteria ratio), and the plates were centrifuged (300 × g for 8 min at 20°C). For indicated wells Cytochalasin D (10 μg/ml) was added for 30 min to eliminate phagocytosis and *S. anginosus* were co-cultured for 3 h, 5 % CO_2.

Micrococcal nuclease (MNase) (1U/ml) was added in order to detach NETs from neutrophils surface. Next, cells were serially diluted in PBS

and seeded in Columbia agar with 5 % sheep blood, and colonies were counted after incubation at 37°C for 48 h.

3.8. NET-mediated bacterial killing

A suspension of *S. anginosus* in DMEM (without phenol red) was added to 5×10^5 PMN/well seeded in DMEM in 96-well plates priory coated with 0.01 mg/ml poly-L-lysine (Sigma- Aldrich) and the plates were centrifuged (300 × g for 8 min at 20°C). Then, neutrophils were stimulated at 37°C with phorbol ester (PMA; Sigma-Aldrich) 25 nM for 3 hours. After that time, 1 U/ml of MNase was added and incubated for 15 minutes at room temperature. Then plates were centrifuged at 1800 × g, 10 min, 21°C. Extruded NETs were collected and incubated at 37°C with *S. anginosus* with or without the addition of DNase (100 U/ml) at a MOI of 1:5 (based on the number of neutrophils from which the NETs were collected). After 3 h, bacterial survival was estimated by plating dilutions on blood Columbia agar plates and counting colonies of bacteria.

3.9. Microscopic imaging

NETs visualisation was described by our team previously (Bryzek et al., 2019). Neutrophils were plated at $5\times$ 10^5 cells on poly-L-lysine-coated coverslips. After 30 min of incubation at 37°C, the cells were left untreated or stimulated with the PMA (25 nM) as a positive control, different strains of *S. anginosus*, or *S. pyogenes* as a reference, at a MOI of 1:5, by 1 h and 3 h. Cells were stained with antibodies rabbit anti-human neutrophil elastase (NE; Athens Research and Technology, USA) followed by APC-conjugated goat anti-rabbit IgG F(ab)2 (Jackson ImmunoResearch Laboratories, USA). Cells were counterstained with 1 μg/ml Hoechst 33342 (Invitrogen/ThermoFisher Scientific), a DNA-intercalating dye. Cells were stained with antibodies rabbit anti-human neutrophil elastase (NE; Athens Research and Technology, USA) for 1 h, followed by APC-conjugated goat anti-rabbit IgG F(ab)2 (Jackson ImmunoResearch Laboratories, USA) for 45 min. Cells were counterstained with 1 μg/ml Hoechst 33342 (Invitrogen/ThermoFisher Scientific). The survival of bacteria in contact with NETs was examined using the LIVE/DEAD BacLight kit (Molecular Probes). NETs were generated by PMN stimulated with PMA as described above. Next *S. anginosus* strain was added in MOI 1:10. The staining procedure was performed according to the manufacturer's instructions. Bacteria were visualized by fluorescent microscopy. The quantification of the NETs length was performed using ImageJ software.

3.10. Galleria mellonella infection model

For the evaluation of *S. anginosus* virulence properties, we used the infection model of *G. melonella.* The *G. mellonella* larvae were purchased from Biosystems Technology and stored in the dark at 17°C. Only healthy larvae with no signs of melanization were used in the experiments. Ten larvae per group were infected by injection into the last proleg using a Hamilton syringe with 10 μL of bacterial inoculum containing from 10^7 CFU of *S. anginosus*. Ten microliters of PBS was used as a control. The larvae were incubated at 37°C in 9-cm Petri dishes without food. Their condition in terms of activity and melanization was monitored up to 48 h after infection and scored as follow: Activity: 0- move without stimulation, 1- move after stimulation, 2- minimal movement on stimulation, 3- no movement; Melanization: 0- no melanization, 1- spots on beige larvae, slightly marked tail line, 2- tall line on beige larvae, 3- brown larvae. The larvae were considered dead when they did not move in response to tactile stimulation. Method was described recently (Budziaszek et al., 2023). Larvae were infected by injection with 10 μL of *S. anginosus* inoculum containing 10^7 CFU. The procedure of hemocytes collection and staining was adopted from previous studies (Tsai et al., 2016; Chen and Keddie, 2021). To collect larval haemolymph, larvae were wiped with 70 % ethanol and then an incision was made on the proleg with a scalpel. hemolymph was mixed with the ice-cold PBS buffer with 0.36 % β-mercaptoethanol to prevent coagulation and melanization and placed onto polylysine slides. The slides were incubated in the 37/CO_2 for 30 minutes to allow the cells to settle. After that time the supernatant was the supernatant was discarded. The bacteria in haemolymph were examined using the LIVE/DEAD BacLight kit (Molecular Probes). The staining procedure was performed according to the manufacturer's instructions. At the end the preparations were closed with mounting medium with DAPI. Bacterial survival/proliferation in *G. mellonella* larvae was controlled by homogenization larvae infected with bacteria after 0 h and 48 h. The samples were serially diluted in PBS and plated on Columbia agar with 5 % sheep blood, and colonies were counted after incubation at 37°C for 48 h. As a control, PBS-injected larvae were used in an analogous procedure.

3.11. Co-infection studies

The influence of highly active *S. anginosus* 3792/10 strain on the survival of selected pathogens (*E.c, S.e, K.p, E.f*) in the presence of PMN was examined. For this purpose, human neutrophils were seeded at 2×10^6/well in 0.01 mg/ml poly-L-lysine-coated 24-well plates and centrifuged (200 × *g*, 5 min) to allow cells to adhere to the plates. Then, neutrophils were stimulated with 25 nM PMA for 3 h at 37°C. Extruded NETs were collected and incubated at 37°C with pathogen cultures (PMN:pathogen, 1:2) or a mixture of pathogen with *S. anginosus* suspension (PMN:Pathogen:*S.ang*, 1:2:5 or 1:2:50) were added to the stimulated PMNs. Co-incubation was carried out at 37°C, 5 % CO_2 for 2 h. After this time, the cultures were plated using the serial dilution method on agar plates dedicated to pathogens, and the colonies were counted. For *G. mellonella* coinfection studies *S. anginosus* 3792/10 at dose 10^7 CFU was mixed with *E coli* at dose 10^6 CFU and injected to *G. mellonella.* After 24 h larvae were homogenized. The samples were serially diluted in PBS and plated on McConkey agar. Colonies were counted after incubation at 37°C for 24 h.

3.12. Statistical analysis

Data were analysed using GraphPad Prism version 9.1.1 (GraphPad Software). Parametric tests (unpaired Student's t-test or analysis of variance [ANOVA] and Pearson correlation coefficients) were used. A P value of < 0.05 was used for statistical significance. The logarithmic rank test (Mantel-Cox) was used for survival analyses.

CRediT authorship contribution statement

Joanna Koziel: Writing – review & editing, Writing – original draft, Validation, Supervision, Software, Resources, Project administration, Methodology, Investigation, Funding acquisition, Formal analysis, Data curation, Conceptualization. **Michal Dmowski**: Investigation. **Izabela Kern-Zdanowicz**: Writing – review & editing, Methodology, Investigation, Funding acquisition. Aleksandra Kozinska: Investigation. **Izabela Sitkiewicz**: Writing – review & editing, Funding acquisition, Conceptualization. **Keerthanaa Nandagopal**: Methodology, Investigation. **Aleksandra Kurylek**: Investigation. **Magdalena Pilarczyk-Zurek**: Writing – review & editing, Writing – original draft, Visualization, Methodology, Investigation, Formal analysis, Data curation, Conceptualization. **Joanna Budziaszek**: Visualization, Methodology, Investigation

Acknowledgements

The study was funded by the National Science Center, Poland, grant no. 2018/29/B/NZ6/00624.

The funders had no role in study design, data collection, and analysis, decision to publish, or preparation of the manuscript. All authors declared that they have no conflict of interest to disclose.

Appendix A. Supporting information

Supplementary data associated with this article can be found in the online version at doi:10.1016/j.micres.2024.127959.

Data availability

Data will be made available on request.

References

Ajit, A., Jacob, B., Warrier, A., 2023. Coinfection of streptococcus agalactiae and tuberculous osteomyelitis of tibia mimicking brodie's abscess in an immunocompetent adult: a case report. J. Orthop. Case Rep. 13 (7), 95.

Al Majid, F., et al., 2020. Streptococcus anginosus group infections: management and outcome at a tertiary care hospital. J. Infect. Public Health 13 (11), 1749–1754.

Altschul, S.F., et al., 1990. Basic local alignment search tool. J. Mol. Biol. 215 (3), 403–410.

Asam, D., Spellerberg, B., 2014. Molecular pathogenicity of S treptococcus anginosus. Mol. Oral. Microbiol. 29 (4), 145–155.

Brinkmann, V., et al., 2004. Neutrophil extracellular traps kill bacteria. Science 303 (5663), 1532–1535.

Browne, N., Heelan, M., Kavanagh, K., 2013. An analysis of the structural and functional similarities of insect hemocytes and mammalian phagocytes. Virulence 4 (7), 597–603.

Bryzek, D., et al., 2019. Triggering NETosis via protease-activated receptor (PAR)-2 signaling as a mechanism of hijacking neutrophils function for pathogen benefits. PLoS Pathog. 15 (5), e1007773.

Buchanan, J.T., et al., 2006. DNase expression allows the pathogen group A Streptococcus to escape killing in neutrophil extracellular traps. Curr. Biol. 16 (4), 396–400.

Budziaszek, J., et al., 2023. Studies of Streptococcus anginosus Virulence in Dictyostelium discoideum and Galleria mellonella Models. Infect. Immun. 91 (5), e00016–e00023.

Camacho, C., et al., 2009. BLAST+: architecture and applications. BMC Bioinforma. 10, 1–9.

Chalmers, C., et al., 2020. Streptococcus pyogenes nuclease A (SpnA) mediated virulence does not exclusively depend on nuclease activity. J. Microbiol., Immunol. Infect. 53 (1), 42–48.

Chang, A., et al., 2011. Functional analysis of Streptococcus pyogenes nuclease A (SpnA), a novel group A streptococcal virulence factor. Mol. Microbiol. 79 (6), 1629–1642.

Chen, R.Y., Keddie, B.A., 2021. Galleria mellonella (Lepidoptera: Pyralidae) hemocytes release extracellular traps that confer protection against bacterial infection in the hemocoel. J. Insect Sci. 21 (6), 17.

Cherny, K.E., Sauer, K., 2019. Pseudomonas aeruginosa requires the DNA-specific endonuclease EndA to degrade extracellular genomic DNA to disperse from the biofilm. J. Bacteriol. 201 (18), 10.1128/jb.00059-19.

Cumley, N.J., et al., 2012. The CovS/CovR acid response regulator is required for intracellular survival of group B Streptococcus in macrophages. Infect. Immun. 80 (5), 1650–1661.

Derré-Bobillot, A., et al., 2013. N uclease A (Gbs 0661), an extracellular nuclease of S treptococcus agalactiae, attacks the neutrophil extracellular traps and is needed for full virulence. Mol. Microbiol. 89 (3), 518–531.

Doke, M., et al., 2017. Nucleases from Prevotella intermedia can degrade neutrophil extracellular traps. Mol. Oral. Microbiol. 32 (4), 288–300.

Fu, K., et al., 2024. Streptococcus anginosus promotes gastric inflammation, atrophy, and tumorigenesis in mice. Cell 187 (4), 882–896 e17.

Furuichi, M., Horikoshi, Y., 2018. Sites of infection associated with Streptococcus anginosus group among children. J. Infect. Chemother. 24 (2), 99–102.

Garcia Gonzalez, J., Hernandez, F.J., 2022. Nuclease activity: an exploitable biomarker in bacterial infections. Expert Rev. Mol. Diagn. 22 (3), 265–294.

Jacobs, J., Stobberingh, E., 1995. Hydrolytic enzymes of Streptococcus anginosus, Streptococcus constellatus and Streptococcus intermedius in relation to infection. Eur. J. Clin. Microbiol. Infect. Dis. 14, 818–820.

Jiang, S., et al., 2020. Clinical characteristics of infections caused by Streptococcus anginosus group. Sci. Rep. 10 (1), 9032.

Junckerstorff, R.K., Robinson, J.O., Murray, R.J., 2014. Invasive Streptococcus anginosus group infection—does the species predict the outcome? Int. J. Infect. Dis. 18, 38–40.

Juneau, R.A., et al., 2015. A thermonuclease of Neisseria gonorrhoeae enhances bacterial escape from killing by neutrophil extracellular traps. J. Infect. Dis. 212 (2), 316–324.

von Köckritz-Blickwede, M., Blodkamp, S., Nizet, V., 2016. Interaction of bacterial exotoxins with neutrophil extracellular traps: impact for the infected host. Front. Microbiol. 7, 188046.

Lau, H.Y., Clegg, S., Moore, T.A., 2007. Identification of Klebsiella pneumoniae genes uniquely expressed in a strain virulent using a murine model of bacterial pneumonia. Microb. Pathog. 42 (4), 148–155.

Liao, C., et al., 2022. Pathogen-derived nucleases: an effective weapon for escaping extracellular traps. Front. Immunol. 13, 899890.

Maguin, E., et al., 1996. Efficient insertional mutagenesis in lactococci and other gram-positive bacteria. J. Bacteriol. 178 (3), 931–935.

Meijer, M., et al., 2012. Experimental immunology Extracellular Traps: How to isolate and quantify extracellular DNA (ET-DNA). Cent. Eur. J. Immunol. 37 (4), 321–325.

Mónaco, A., et al., 2021. Salmonella typhimurium triggers extracellular traps release in murine macrophages. Front. Cell. Infect. Microbiol. 11, 639768.

Mücke, M.M., et al., 2017. The role of Enterococcus spp. and multidrug-resistant bacteria causing pyogenic liver abscesses. BMC Infect. Dis. 17, 1–10.

Noguchi, S., et al., 2015. The clinical features of respiratory infections caused by the Streptococcus anginosus group. BMC Pulm. Med. 15, 1–9.

Noguchi, S., et al., 2021. Association between obligatory anaerobes and empyema caused by Streptococcus anginosus group bacteria. Respir. Investig. 59 (5), 686–690.

Obszańska, K., et al., 2016. Group Strains Isolated in Poland (1996–2012) and their Antibiotic Resistance Patterns. Pol. J. Microbiol. 65 (1), 33–41.

Pilarczyk-Zurek, M., Sitkiewicz, I., Koziel, J., 2022. The clinical view on Streptococcus anginosus group: opportunistic pathogens coming out of hiding. Front Microbiol 13, 956677.

Ricci, M.L., et al., 1994. Electrotransformation of Streptococcus agalactiae with plasmid DNA. FEMS Microbiol. Lett. 119 (1-2), 47–52.

Ríos-López, A.L., et al., 2021. Avoiding the trap: mechanisms developed by pathogens to escape neutrophil extracellular traps. Microbiol. Res. 243, 126644.

Schüler, V., et al., 2012. Glycan-binding specificities of Streptococcus mutans and Streptococcus sobrinus lectin-like adhesins. Clin. Oral. Investig. 16, 789–796.

Sharma, P., et al., 2019. Nucleases of bacterial pathogens as virulence factors, therapeutic targets and diagnostic markers. Int. J. Med. Microbiol. 309 (8), 151354.

Shinzato, T., Saito, A., 1994. A mechanism of pathogenicity of "Streptococcus milleri group" in pulmonary infection: synergy with an anaerobe. J. Med. Microbiol. 40 (2), 118–123.

Shinzato, T., Saito, A., 1995. The Streptococcus milleri group as a cause of pulmonary infections. Clin. Infect. Dis. 21 (ement_3), S238–S243.

Sitkiewicz, I., 2018. How to become a killer, or is it all accidental? Virulence strategies in oral streptococci. Mol. Oral. Microbiol. 33 (1), 1–12.

Speziale, P., Pietrocola, G., 2021. Staphylococcus aureus induces neutrophil extracellular traps (NETs) and neutralizes their bactericidal potential. Comput. Struct. Biotechnol. J. 19, 3451–3457.

Sumby, P., et al., 2005. Extracellular deoxyribonuclease made by group A Streptococcus assists pathogenesis by enhancing evasion of the innate immune response. Proc. Natl. Acad. Sci. 102 (5), 1679–1684.

Teufel, F., et al., 2022. SignalP 6.0 predicts all five types of signal peptides using protein language models. Nat. Biotechnol. 40 (7), 1023–1025.

Tsai, C.J.-Y., Loh, J.M.S., Proft, T., 2016. Galleria mellonella infection models for the study of bacterial diseases and for antimicrobial drug testing. Virulence 7 (3), 214–229.

Wanahita, A., et al., 2002. Interaction between human polymorphonuclear leukocytes and Streptococcus milleri group bacteria. J. Infect. Dis. 185 (1), 85–90.

Wang, Z., et al., 2014. Two novel functions of hyaluronidase from Streptococcus agalactiae are enhanced intracellular survival and inhibition of proinflammatory cytokine expression. Infect. Immun. 82 (6), 2615–2625.

Whiley, R.A., et al., 2014. Differential potentiation of the virulence of the Pseudomonas aeruginosa cystic fibrosis liverpool epidemic strain by oral commensal Streptococci. J. Infect. Dis. 209 (5), 769–780.

Wilton, M., et al., 2018. Secreted phosphatase and deoxyribonuclease are required by Pseudomonas aeruginosa to defend against neutrophil extracellular traps. Infect. Immun. 86 (9), 10.1128/iai.00403-18.

Yang, H., et al., 2016. New insights into neutrophil extracellular traps: mechanisms of formation and role in inflammation. Front. Immunol. 7, 207281.

Yu, N.Y., et al., 2010. PSORTb 3.0: improved protein subcellular localization prediction with refined localization subcategories and predictive capabilities for all prokaryotes. Bioinformatics 26 (13), 1608–1615.